

Binding of the antibacterial peptide magainin 2 amide to small and large unilamellar vesicles

Torsten Wieprecht, Ognjan Apostolov, Joachim Seelig*

Department of Biophysical Chemistry, Biocenter of the University of Basel, Klingelbergstrasse 70, CH-4056 Basel, Switzerland

Abstract

The thermodynamics of binding of the antibacterial peptide magainin 2 amide (M2a) to negatively charged small (SUVs) and large (LUVs) unilamellar vesicles has been studied with isothermal titration calorimetry (ITC) and CD spectroscopy at 45°C. The binding isotherms as well as the ability of the peptide to permeabilize membranes were found to be qualitatively and quantitatively similar for both model membranes. The binding isotherms could be described with a surface partition equilibrium where the surface concentration of the peptide immediately above the plane of binding was calculated with the Gouy–Chapman theory. The standard free energy of binding was $\Delta G^0 \approx -22$ kJ/mol and was almost identical for LUVs and SUVs. However, the standard enthalpy and entropy of binding were distinctly higher for LUVs ($\Delta H^0 = -15.1$ kJ/mol, $\Delta S^0 = 24.7$ J/molK) than for SUVs ($\Delta H^0 = -38.5$ kJ/mol, $\Delta S^0 = -55.3$ J/molK). This enthalpy–entropy compensation mechanism is explained by differences in the lipid packing. The cohesive forces between lipid molecules are larger in well-packed LUVs and incorporation of M2a leads to a stronger disruption of cohesive forces and to a larger increase in the lipid flexibility than peptide incorporation into the more disordered SUVs. At 45°C the peptide easily translocates from the outer to the inner monolayer as judged from the simulation of the ITC curves. © 2000 Elsevier Science B.V. All rights reserved.

Keywords: Peptide–membrane interaction; Antimicrobial peptide; Amphipathic peptide; Titration calorimetry; Magainin

* Corresponding author. Tel.: +41-61-267-2190; fax: +41-61-267-2189.

E-mail address: joachim.seelig@unibas.ch (J. Seelig).

1. Introduction

Magainins are antimicrobial peptides belonging to the innate immune response of the African clawed frog *Xenopus laevis* [1]. The positively charged peptides act by enhancing the permeability of the microbial target membrane [2,3]. Magainins adopt a random coil conformation in water, but fold into amphipathic α -helices upon binding to the biological membrane [4–6]. Membrane-binding is the first step of the peptide–membrane interaction mechanism and knowledge of its determinants and driving forces is prerequisite for the understanding of the mechanism of action and of the molecular reasons for the prokaryotic specificity. Several membrane-binding studies of magainin peptides have been published [4,6–9]. The positively charged peptides were found to bind preferentially to negatively charged membranes which is a major reason for the prokaryotic specificity. The enhanced affinity is caused by an electrostatic attraction of the peptides to the negatively charged membrane surface rather than a specific peptide–lipid interaction [9].

Membrane binding studies are mostly performed using small unilamellar vesicles (SUVs) made by sonification (mean diameter ~ 30 nm) or large unilamellar vesicles (LUVs) prepared by the extrusion technique (mean diameter ~ 100 nm). SUVs are highly curved and are less densely packed than LUVs. Nevertheless, SUVs offer specific advantages for physical–chemical studies. Because of their small diameter, their light scattering activity is minimal and spectroscopic methods, such as circular dichroism (CD) spectroscopy, can be used to detect changes in the protein conformation upon binding. Furthermore, high-sensitivity isothermal titration calorimetry (ITC) has revealed that the heats of binding obtained with SUVs are often distinctly more exothermic than those obtained with LUVs [10–12]. This effect was designated as non-classical hydrophobic effect [12]. The large binding enthalpy improves the signal-to-noise ratio of the calorimetric measurement and leads to a higher accuracy in the evaluation of the binding isotherms. LUVs, on the other hand, appear to be more

closely related to biological membranes, since the curvature stress is reduced and the lipid packing density is higher. Since both model systems are widely used we have systematically compared the two types of vesicles for the specific case of magainin 2 amide (M2a) binding and membrane permeabilization.

Binding of M2a to negatively charged SUVs composed of 1-palmitoyl-2-oleoyl-*sn*-glycero-3-phosphocholine/1-palmitoyl-2-oleoyl-*sn*-glycero-3-phospho-*rac*-glycerol [POPC/POPG (3:1)] has already been investigated previously at 30°C [8]. The binding isotherm was derived with ITC for peptide concentrations below 7 μ M. At peptide concentrations > 7 μ M, a second, endothermic process was superimposed on the exothermic binding reaction and was tentatively assigned to pore formation. The endothermic process [$\Delta H \approx 25$ kJ/mol (~ 6 kcal/mol) peptide] was found to be dependent on the lipid-to-protein ratio: upon dilution with lipid the ‘pores’ disintegrated, returning the heat consumed during formation. ‘Pore’ formation was clearly visible at 30°C for POPC/POPG (3:1) membranes [8] but barely detectable with pure POPC membranes [9]. In the present study, all measurements were performed at 45°C since the higher temperature should favor the endothermic process. Indeed, the latter appeared to be fully activated at all lipid-to-protein ratios yielding a constant reaction enthalpy for most peptide concentrations measured (up to 40 μ M). This greatly simplified the analysis of the calorimetric titration experiments. The binding isotherms for LUVs and SUVs could thus be determined with ITC. As an additional control, the binding isotherm for SUVs was also measured with CD spectroscopy.

2. Materials and methods

2.1. Materials

POPC and POPG were purchased from Avanti Polar Lipids, Inc, Alabaster, AL, USA. M2a was a kind gift of Dr W.L. Maloy (Magainin Pharmaceuticals, Inc, Plymouth Meeting, PA, USA). All other chemicals were of analytical or reagent

grade. Buffer was prepared from 18 M Ω water obtained from a NANOpure A filtration system. The buffer used in all experiments was 10 mM Tris, 100 mM NaCl at pH 7.4.

2.2. Preparation of vesicles

A defined amount of lipid in chloroform was first dried under nitrogen. The lipid was dissolved in dichloromethane and then again dried under nitrogen and, subsequently, overnight under high vacuum. Typically, 2–3 ml of buffer (10 mM Tris, 100 mM NaCl, pH 7.4) were added to the lipid and the dispersion was extensively vortexed. For preparation of small unilamellar vesicles (SUVs) the lipid dispersion was sonified (in ice-water) using a titanium tip ultrasonicator until the solution became transparent. Titanium debris was removed by centrifugation (Eppendorf table-top centrifuge, 10 min at 14 000 rev./min).

LUVs were prepared by the extrusion technique [13]. The lipid suspension was frozen and thawed in liquid nitrogen (six times) and extruded through polycarbonate filters (six times through two stacked 0.4- μ m pore size filters followed by eight times through two stacked 0.1- μ m filters). The lipid concentration was calculated on basis of the weight of the dried lipid for SUVs as well as LUVs.

SUVs and LUVs for dye release experiments were prepared as described above using calcein containing buffer (70 mM calcein, 10 mM Tris, pH 7.4). After preparation, the untrapped calcein was removed from the vesicles by gel filtration on a Sephadex G75 column (eluent: buffer containing 10 mM Tris, 100 mM NaCl, pH 7.4). The lipid concentration was determined by quantitative phosphorus analysis [14].

2.3. High sensitivity titration calorimetry

Isothermal titration calorimetry was performed using a MicroCal Omega high-sensitivity titration calorimeter (Microcal, Norhampton, MA) [15]. Solutions were degassed under vacuum prior to use. The calorimeter was calibrated electrically. The heats of dilution were determined in control experiments by injecting either peptide solution

or lipid suspension into buffer. The heats of dilution were subtracted from the heats determined in the corresponding peptide–lipid binding experiments.

2.4. Circular dichroism measurements

CD measurements were carried out on a Jasco 720 spectrometer at wavelengths between 200 and 260 nm at 45°C. Minor contributions of circular dichroism and circular differential scattering of the SUVs were eliminated by subtracting the lipid spectra of the corresponding peptide-free suspensions.

2.5. Dye release experiments

Aliquots of a calcein-containing vesicle suspension (10–20 μ l, depending on the lipid concentration) were injected into a cuvette containing 2.0 ml of a stirred, thermostated peptide solution of a defined concentration (final lipid concentration was between 50 and 81 μ M). Calcein release from vesicles was determined fluorometrically by measuring the decrease in self-quenching (excitation at 490 nm, emission at 520 nm) on a Jasco FP 777 spectrofluorometer. The fluorescence intensity corresponding to 100% calcein release was determined by addition of 100 μ l of 10% Triton X-100 solution.

3. Results

3.1. ITC experiments

Binding isotherms of M2a to POPC/POPG (3:1) LUVs at 45°C were determined by injecting lipid vesicles into peptide solutions [16]. In this type of experiment, small aliquots of a concentrated vesicle solution (6 μ l of 35 mM lipid) were injected into the calorimeter cell containing the peptide solution (between 6 and 40 μ M M2a). Calorimetric traces of typical experiments are given in Fig. 1 (upper panels). Fig. 1a,c show the results of injection of 6 μ l of 35 mM LUVs into 6 and 40 μ M M2a, respectively, and Fig. 1b,d show the analog experiments performed with SUVs.

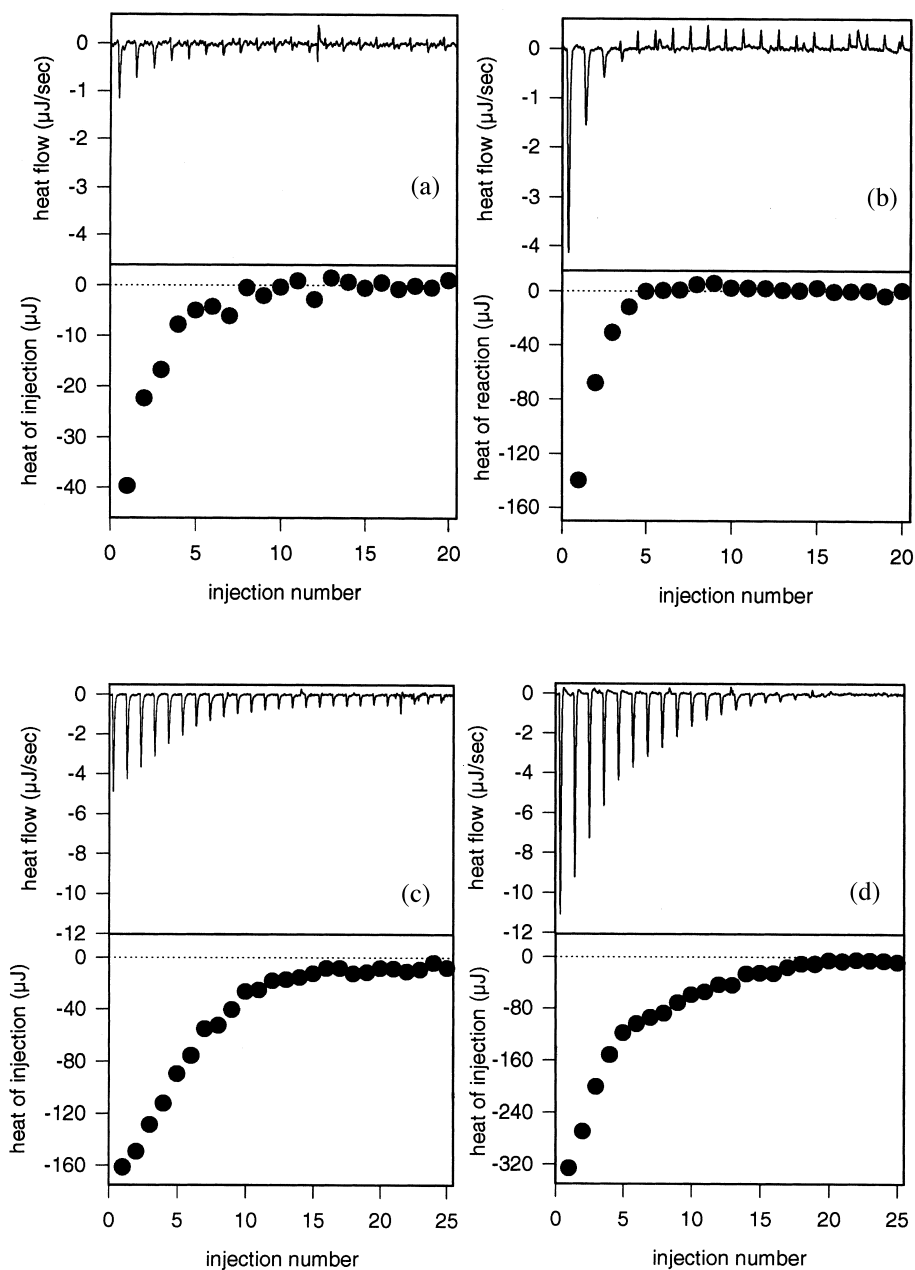


Fig. 1. Titration calorimetry of M2a solutions with POPC/POPG (3:1) LUVs (a,c) and SUVs (b,d) at 45°C (buffer: 10 mM Tris, 100 mM NaCl, pH 7.4). The upper panels show the calorimeter tracings and the lower panels show the heats of injection. The heat of dilution was measured in separate control experiments and is already subtracted from the heats of injection. The specific conditions were as follows: (a) Injection of 6- μ l aliquots of 35 mM LUVs into 6 μ M M2a. (b) Injection of 6- μ l aliquots of 35 mM SUVs into 6 μ M M2a. (c) Injection of 6- μ l aliquots of 35 mM LUVs into 40 μ M M2a. (d) Injection of 6- μ l aliquots of 35 μ M SUVs into 40 μ M M2a.

Control experiments with injection of lipid into buffer revealed small and constant heats of dilution which were subtracted from the actual measurement. The corrected heats of injections are given in the lower panels of Fig. 1a–d. Binding of M2a to vesicles was always accompanied by exothermic heats of reaction. These were considerably smaller for LUVs (Fig. 1a,c), but the relative change of the exothermic heats with increasing injection number was comparable for LUVs and for SUVs. The measured heats, per injection, h_i , are expected to decrease in magnitude with increasing injection number since less and less peptide remains free in solution.

The ITC experiments provide the standard molar reaction enthalpy ΔH^0 according to

$$\Delta H^0 = \sum_i \delta h_i / (c_{\text{pep}}^0 V_{\text{cell}}) \quad (1)$$

where δh_i are the heats of injection (heats of dilution subtracted), c_{pep}^0 is the total peptide concentration and V_{cell} is the volume of the calorimeter cell (1.3353 ml) [16]. ΔH^0 was found to be -15.1 ± 3.3 kJ/mol for LUVs (number of experiments $n = 9$) and -38.5 ± 2.5 kJ/mol for SUVs ($n = 8$) (Table 1). Obviously, binding of M2a to SUVs is distinctly more exothermic than binding to LUVs.

Next, the binding isotherms $X_b = f(c_f)$ (X_b = molar ratio of bound peptide per total lipid, c_f = peptide equilibrium concentration free in solution) can be derived from the measured δh_i [8,16]

and are shown in Fig. 2. The binding isotherms are based on the assumption that the lipid on both leaflets of the vesicles was accessible to the peptide. The two isotherms are the results of nine LUV and eight SUV lipid-into-peptide titration experiments performed at different peptide concentrations between 6 and 40 μM . Very similar binding isotherms were found for LUVs and SUVs, indicating a slightly better binding of M2a to LUVs than to SUVs.

The theoretical analysis of the binding isotherms requires the assumption of a specific binding model. The model employed here is a *surface partition* equilibrium with the additional condition that the amount of bound peptide is linearly related to the peptide concentration immediately above the membrane surface (*surface* concentration, c_M) and *not* to the *bulk* concentration, c_f :

peptide (membrane–water interface)

\rightleftharpoons peptide (membrane-bound)

$$X_b = K c_M \quad (2)$$

c_M depends on: (i) the free peptide concentration in bulk solution, c_f ; (ii) on the peptide charge; and (iii) on the membrane surface potential. POPC/POPG (3:1) vesicles are characterized by a negative surface potential of approximately -50 mV in the present buffer leading to an attraction

Table 1
Thermodynamic parameters of binding of M2a to POPC/POPG (3:1) vesicles at 45°C

	ΔH^0 ^a (kJ/mol)	K ^b (M ⁻¹) ^b	ΔG^0 ^c (kJ/mol)	$-T\Delta S^0$ ^d (kJ/mol)	ΔS^0 (J/molK)
LUVs	-15.1	110	-23.0	-7.9	25.0
SUVs	-38.5	50	-20.9	17.6	-55.3
LUVs coil ^e	29.8		-14.2	-44.0	138.4
SUVs coil ^e	6.4		-12.1	-18.5	58.2

^a ΔH^0 as directly observed in the ITC experiments.

^b K was calculated from the ITC and CD binding isotherms as described in the text.

^c $\Delta G^0 = RT \ln 55.5 K$.

^d $-T\Delta S^0 = \Delta G^0 - \Delta H^0$.

^eBinding parameters for a hypothetical M2a peptide which binds to the membrane without undergoing the coil \rightarrow α -helix transition.

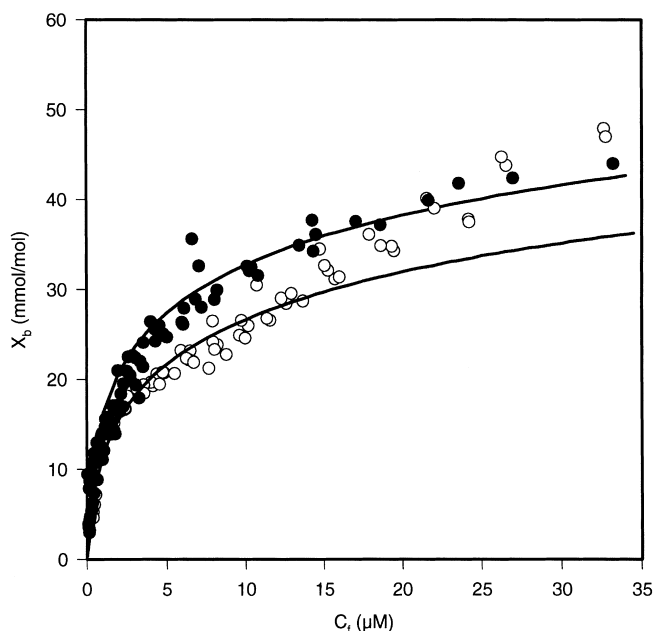


Fig. 2. Binding isotherms of M2a for POPC/POPG (3:1) LUVs (●) and SUVs (○) at 45°C (buffer 10 mM Tris, 100 mM NaCl, pH 7.4). The binding isotherms are based on nine (LUVs) and eight (SUVs) independent lipid into peptide titrations with peptide concentrations between 6 and 40 μM . The ratio of bound peptide per lipid, X_b , is calculated on the basis of the lipid present in the outer and inner layer of the vesicles. The solid lines correspond to theoretical binding isotherms with $K = 110 \text{ M}^{-1}$ (LUVs) and $K = 50 \text{ M}^{-1}$ (SUVs), calculated by combining a surface partition equilibrium with the Gouy–Chapman theory.

of the cationic M2a ($z \approx 3.8$ – 3.6 , depending on the surface concentration) from bulk solution to the membrane surface. Consequently, the peptide concentration near the membrane surface (c_M) is enhanced compared to that in bulk solution (c_f). Using the Gouy–Chapman theory (for reviews see Aveyard and Haydon [17] and McLaughlin [18,19]) it is possible to calculate c_M for each data point of the binding isotherm and to determine the binding constant K . A detailed description of this binding model as applied to magainin peptides can be found elsewhere [8,9]. Using this model we have simulated the calorimetric curves obtained for the injection of POPC/POPG (3:1) vesicles into 6 μM M2a (lowest peptide concentrations, Fig. 3). Good agreement was found for $K = 30 \text{ M}^{-1}$, $z = 3.6$ – 3.7 , $\Delta H^0 = -12.6 \text{ kJ/mol}$ for LUVs (Fig. 3a) and $K = 50 \text{ M}^{-1}$, $z = 3.6$ – 3.7 , $\Delta H^0 = -37.7 \text{ kJ/mol}$ for SUVs (Fig. 3b). The calculations were performed with the assumption that the peptide can cross the bilayer (100% of lipid accessible for binding). The binding con-

stants are consistent with those recently reported for binding of M2a to POPC/POPG (3:1) SUVs at 30°C ($K = 50 \text{ M}^{-1}$) [8].

Finally, we have used this model to simulate the binding isotherms up to $c_f = 35 \mu\text{M}$. Fig. 2 demonstrates that the binding isotherm for LUVs at 45°C can be described by the surface partition model extremely well with $K = 110 \text{ M}^{-1}$. For SUVs a good fit is obtained with $K = 50 \text{ M}^{-1}$ up to an equilibrium concentration of $C_{\text{pep}} \sim 15 \mu\text{M}$. For both calculations it was assumed that the peptide can cross the membrane and that all lipid is available for binding.

The standard free energy of binding, ΔG^0 , can be calculated from K using the relation

$$\Delta G^0 = -RT \ln [(55.5 \text{ M})K] \quad (3)$$

where the factor 55.5 M is the molar concentration of water and corrects for the cratic contribution [20]. ΔG^0 was found to be -23 kJ/mol for

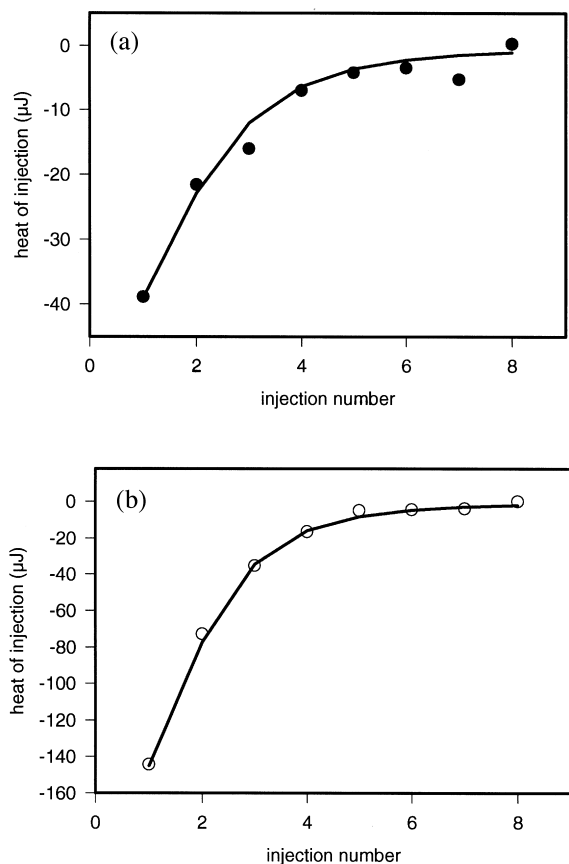


Fig. 3. Heat of injection as a function of the injection number for (a) the injection of 35 mM POPC/POPG (3:1) LUVs into 6 μ M M2a; and (b) the injection of 35 mM POPC/POPG (3:1) SUVs into 6 μ M M2a. The solid lines correspond to the best fit of the experimental data points using a model which combines a surface partition equilibrium with the Gouy-Chapman theory. The specific fit parameters are (a) $K = 30 \text{ M}^{-1}$, $z = 3.6\text{--}3.7$, $\Delta H^0 = -12.6 \text{ kJ/mol}$; and (b) $K = 50 \text{ M}^{-1}$, $z = 3.6\text{--}3.7$, $\Delta H^0 = -37.7 \text{ kJ/mol}$.

LUVs and -20.9 kJ/mol for SUVs and corresponds to the free energy of transfer of peptide from the lipid–water interface (peptide concentration c_M) into the lipid bilayer.

The standard entropy of binding can be calculated according to $\Delta S^0 = (\Delta H^0 - \Delta G^0)/T$ and was negative for POPC/POPG (3:1) SUVs (-55.3 J/molK) but positive for LUVs (25.0 J/molK). While the entropy drives binding of M2a to LUVs it opposes binding to SUVs. The thermodynamic binding parameters are summarized in Table 1.

3.2. CD spectroscopy

Binding isotherms can be derived easily from ITC measurements if ΔH is constant and independent of X_b . This is normally observed for lipid-into-peptide titrations at a low peptide concentration and hence low X_b values. For higher peptide concentrations, changes in the structure of the membrane and also peptide–peptide interactions may occur, which could result in a ΔH which varies with the extent of peptide binding. In order to verify the ITC-derived binding isotherms, we have therefore measured M2a binding isotherms to SUVs also with CD spectroscopy (at 45°C).

M2a in solution shows a random coil structure, whereas M2a bound to SUVs is α -helical. CD spectra of a M2a solution ($c_{\text{pep}}^0 = 30 \text{ } \mu\text{M}$) were recorded in presence of varying amounts of POPC/POPG (3:1) SUVs (lipid concentration between 0 and 6 mM). Without lipid, the measured ellipticity reflects the conformation of the peptide in aqueous solution (Θ_W). The ellipticity becomes distinctly more negative with increasing lipid concentration, c_L , and approaches a constant level at a lipid-concentration of $\sim 5 \text{ mM}$ (spectra not shown). At lipid concentrations $> 5 \text{ mM}$ the peptide is completely membrane-bound and characterized by the ellipticity, Θ_M .

At other lipid-to-peptide ratios the fraction of bound peptide, $X_{P,b}$ can be calculated according to

$$X_{P,b} = (\Theta - \Theta_W) / (\Theta_M - \Theta_W) \quad (4)$$

where Θ is the measured ellipticity. Numerical values used for Θ_M and Θ_W in this study were $\Theta_M = -463\,000 \text{ deg cm}^2/\text{dmol}$ and $\Theta_W = -34\,500 \text{ deg cm}^2/\text{dmol}$. The concentration of peptide remaining free in solution, c_f , is

$$c_f = c_{\text{pep}}^0 (1 - X_{P,b}) \quad (5)$$

The molar ratio of bound peptide per lipid, X_b , is given by

$$X_b = c_b / c_L^0 = X_{P,b} c_{\text{pep}}^0 / c_L \quad (6)$$

where c_L^0 is the total lipid concentration.

In Fig. 4 the binding isotherm measured by CD spectroscopy is compared to that obtained from isothermal titration calorimetry (both isotherms calculated on the basis of total lipid). A good agreement between the two methods is obtained. The solid line represents the theoretical binding isotherm calculated with $K = 50 \text{ M}^{-1}$. The CD data follow the theoretical model up to the highest peptide concentration. The present measurements are also consistent with a CD-derived binding isotherm obtained previously at 23°C [6].

3.3. Membrane permeabilization experiments

In order to compare the ability of M2a to permeabilize POPC/POPG (3:1) SUVs and LUVs, we have performed calcein release experiments. The calcein fluorescence within these vesicles is highly self-quenched because of the large dye concentration (70 mM). The addition of a M2a solution to the dye-containing SUVs or

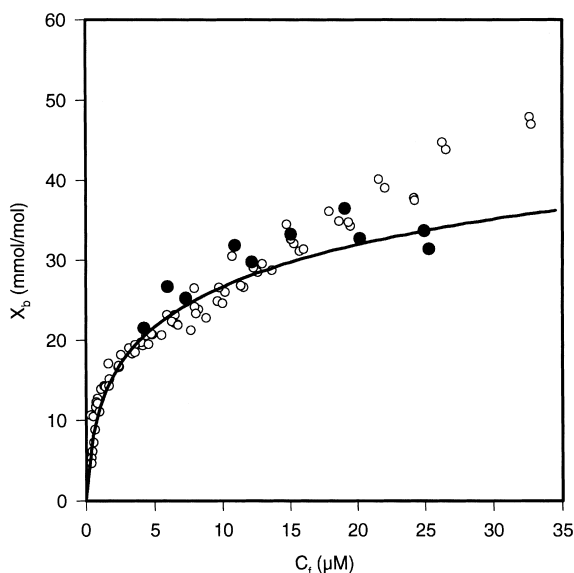


Fig. 4. Comparison between CD-derived binding isotherm (●) and ITC based binding isotherm (○) of M2a to POPC/POPG (3:1) SUVs at 45°C. Binding isotherms were calculated with the assumption that the inner and outer lipid layer is peptide accessible. The solid line corresponds to a theoretical binding isotherm calculated with $K = 50 \text{ M}^{-1}$.

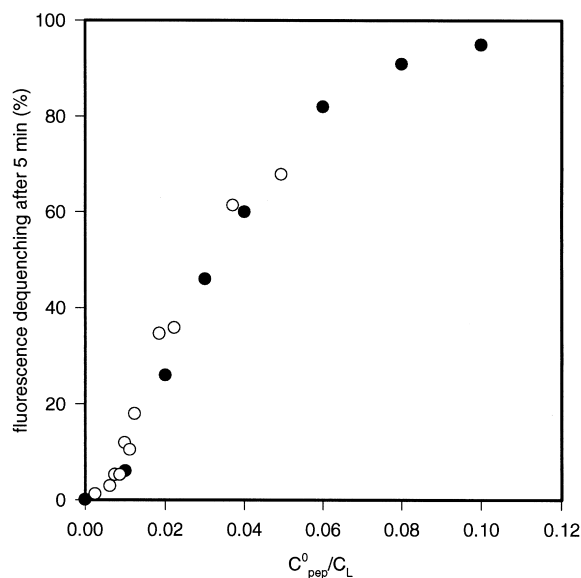


Fig. 5. Dependence of the extent of calcein leakage from POPC/POPG (3:1) LUVs (●) and SUVs (○) on the molar ratio of peptide per lipid. Leakage is given as the percentage of fluorescence dequenching after 5 min. The lipid concentration was 50 μM for LUVs and 81 μM for SUVs.

LUVs at 30°C induces dye release. Dye release leads to a fluorescence dequenching and is reflected in a fluorescence increase. Fig. 5 shows the extent of fluorescence dequenching, measured 5 min after mixing of peptide with POPC/POPG (3:1) vesicles as a function of the total peptide-to-lipid ratio. Virtually no differences are seen between SUVs and LUVs.

4. Discussion

M2a binding to POPC/POPG (3:1) SUVs and LUVs was found to be rather similar but not exactly identical. The binding isotherm could be described by a surface partition equilibrium with proper correction of electrostatic effects by means of the Gouy–Chapman theory [8,21] and a rapid permeation of the peptide through the membrane. The binding isotherms and the free energy of binding were almost identical for LUVs and SUVs. Likewise, the ability of M2a to permeabilize SUVs and LUVs, as assessed by dye efflux

experiments, was virtually identical. Both model systems are hence equally suited to study quantitatively the extent of peptide–membrane binding as well as membrane permeabilization. Binding constants which were similar for SUVs and LUVs have previously been reported for a somatostatin analogue [10] and for amphipathic model peptides [11]. However, the contributions of enthalpy and entropy to the free energy were always distinctly different for LUVs and SUVs. This also holds true for the present study. M2a binding to LUVs is *driven* by entropy (25.0 J/molK), whereas binding to SUVs is *opposed* by entropy (−55.3 J/molK). In contrast, the reaction enthalpy change is more favorable for SUVs (−38.5 kJ/mol) than for LUVs (−15.1 kJ/mol).

4.1. Molecular interpretation of thermodynamic binding parameters

Binding of the positively charged M2a to a negatively charged membrane is a multi-step process. First, the peptide is electrostatically accumulated at the surface of the negatively charged membrane. The extent of the accumulation depends on the peptide charge and the membrane surface potential, where the latter is determined, in turn, by the surface charge density of the membrane and the ionic strength of the solution. Secondly, the peptide is transferred from the membrane surface into the membrane. Thirdly, membrane incorporation is accompanied by a conformational transition of M2a from a random coil structure to an α -helix [4–6]. Finally, the peptide could flip from the outer to the inner monolayer. Since our binding model corrects for the electrostatic accumulation by using surface concentrations, the thermodynamic parameters summarized in Table 1 reflect the sum of the last three steps.

Three energy contributions describe the interaction of M2a with the bilayer membrane: the hydrophobic effect, the coil-to-helix transition, and contributions arising from structural changes within the bilayer itself, including the non-classical hydrophobic effect [9,12,22]. The hydrophobic effect is an entropy-driven process [23]. Partition of non-polar residues into the membrane is ac-

companied by a release of ordered water from the hydrophobic surface increasing thereby the entropy of the system. Despite small structural differences between SUVs and LUVs with respect to lipid packing density and curvature strain it is reasonable to assume that the amount of water released from the peptide side chains upon membrane binding is comparable for both systems.

A second energy contribution to the binding process comes from the coil \rightarrow α -helix transition. CD measurements of M2a and M2a analogs with substituted D-amino acids bound to SUVs revealed that the helix is extended over the whole amino acid chain [6]. Likewise, solid state ^{15}N -NMR experiments reported a completely helical conformation for M2a bound to planar bilayers [5]. Therefore, significant conformational differences between M2a bound to SUVs and LUVs do not exist and helix formation can be expected to make the same energetic contributions to the binding parameters of SUVs and LUVs. We have recently determined the thermodynamic parameters of helix formation of M2a in a membrane environment [22]. Helix formation was found to be driven by an enthalpy change of −3.0 kJ/mol residue (−0.72 kcal/mol residue) and contributed −0.59 kJ/mol residue (−0.14 kcal/mol residue) to the free energy of binding. It is instructive to apply these parameters (determined at 30°C for SUVs), to the present data measured at 45°C. The helicity of M2a in the membrane-bound state as calculated from the mean residue ellipticity at 222 nm is $\sim 65\%$ at 45°C [24]. The contribution of helix formation to the thermodynamic binding parameters is then $\Delta H_{\text{helix}} \sim 0.65 \times 23 \times (-3.0) = -44.9$ kJ/mol and, similarly, $\Delta G_{\text{helix}} \sim -8.8$ kJ/mol. Subtraction of ΔH_{helix} and ΔG_{helix} from the measured results yields the binding parameters of a hypothetical peptide, locked into its coil conformation (designated as LUVs coil and SUVs coil in Table 1). Interestingly, peptide binding *without folding* is driven by entropy but opposed by enthalpy for both, LUVs and SUVs. The favorable entropy change can in part be attributed to the hydrophobic effect. It should be noted that the unfavorable enthalpy change of the hypothetical random coil structure is clearly larger for LUVs (+29.8 kJ/mol) than for SUVs (+6.4

kJ/mol) reflecting presumably differences in the packing density of the two membranes.

Membrane-bound M2a is oriented parallel to the membrane surface with the hydrophilic groups being in contact with the hydrophilic headgroup environment and the hydrophobic groups penetrating into the hydrophobic acyl chain region [5,25]. Because of the superficial peptide location, M2a binding increases the area available for the lipid acyl chains close to the bound peptide. Area expansion results in a membrane thinning, as was recently confirmed for M2a by neutron scattering experiments [26]. Using standard thermodynamic relations it can be shown that the inner energy and the entropy of a bilayer vary considerably with the lipid area, A_L , while the free energy is only little dependent on A_L [10,27,28]. The change in the inner energy U accompanying (reversible) expansion of a bilayer at constant temperature is given by

$$\begin{aligned} (\delta U / \delta A_L)_T &= -\pi + (\delta Q / \delta A_L)_T \\ &= -\pi + T\alpha / \chi = \pi_i \end{aligned} \quad (7)$$

where π is the surface pressure, δQ is the heat of expansion, α is the area expansivity at constant membrane tension, χ is the isothermal area compressibility and π_i is the internal tension. As previously suggested for binding of a somatostatin analogue to vesicles [10], we make the following two assumptions: (i) Binding of M2a to bilayers slightly increases the area per lipid A_L . (ii) The internal tension π_i , which is a measure for the cohesive forces in a sample, is higher in well-packed LUVs than in highly curved SUVs. Typical values of π_i in membranes have been estimated as 290–420 mJ/m² [27,28]. Assuming π_i to be approximately 20% larger for LUVs than for SUVs (as suggested by the area dependence of the internal tension observed in monolayer experiments [28]), the difference in the internal tension between LUVs and SUVs amounts to about $\Delta\pi_i \approx -70$ mJ/m². It is now possible to roughly estimate the area increase induced by M2a binding according to

$$\delta A = \Delta\delta U / (\Delta\pi_i \times N_A) \quad (8)$$

where δA is the area increase of the bilayer upon binding of one M2a molecule, $\Delta\delta U$ is the difference between the internal energy changes accompanying binding of M2a to LUVs and SUVs and N_A is the Avogadro constant [10]. It should be mentioned that $\Delta\delta U \sim \Delta\delta Q = \Delta H_{\text{LUVs}} - \Delta H_{\text{SUVs}}$, since the difference between the membrane tension of LUVs and SUVs, $\Delta\pi$, is much smaller than the difference in the internal tension, $\Delta\pi_i$ [cf. Eq. (7)].

Using $\Delta U = \sim 25$ kJ/mol as determined from the ITC experiments, δA is calculated to be approximately 60 Å². Therefore, binding of one M2a molecule to the bilayer increases the area by approximately 60 Å². The calculation depends critically on the magnitude of $\Delta\pi_i$ and should be considered as a rough estimate of δA . The above calculation shows, however, that the differences in ΔH can be explained by the different packing density of SUVs and LUVs.

The differences in the thermodynamic binding parameters between LUVs and SUVs reflect an entropy–enthalpy compensation mechanism. The free energy of binding of M2a is similar for SUVs and for LUVs, but large differences exist in the binding enthalpy and entropy. An explanation can again be sought in the different lipid packing. Relatively strong cohesive forces (large π_i) exist between the lipid molecules. This state is characterized by a comparably low entropy, since the tight packing reduces the motional degrees of freedom. Binding of M2a to LUVs reduces the cohesive forces at the site of incorporation and increases the lipid flexibility resulting in a large enthalpy and entropy increase as observed in the experiments (see Table 1: parameters corrected for conformational effects: LUVs coil). In highly curved SUVs, the packing of the lipid molecules is less ideal giving rise to weaker cohesive forces between the lipid molecules. At the same time, the entropy of the lipid molecules is higher in SUVs since the looser packing enhances the lipid flexibility. Incorporation of M2a into SUVs leads hence to a smaller increase in the enthalpy but, in turn, also to a smaller entropy increase (cf. Table 1: parameters corrected for conformational effects: SUVs coil). In conclusion, the entropy–

enthalpy compensation mechanism can be attributed to differences in the cohesive forces between lipid molecules in both model systems.

4.2. Membrane permeation of M2a at 30 and 45°C

The binding of M2a to lipid vesicles can be described with a surface partition equilibrium combined with the Gouy–Chapman theory [8,9,21]. Previous studies with POPG/POPC membranes were performed at ambient temperature and an excellent agreement between theory and experiment was obtained for low peptide concentrations. Under these conditions, M2a binds to the lipid vesicle outside only. However, if the peptide concentration is increased beyond a critical limit of approximately 7 μM , the peptide translocates also into the inner monolayer as evidenced, in particular, by fluorescence spectroscopy [29]. This process is accompanied by pore formation/lipid perturbation which is characterized by an endothermic heat of reaction of $\Delta H \approx 25$ kJ/mol which distorts the binding isotherm at 30°C [8]. The present data demonstrate that at the higher temperature of 45°C peptide translocation occurs even at low peptide concentrations. The binding isotherms for LUVs and SUVs can be explained with K -values consistent with the previous measurements ($K \sim 50$ – 110 M^{-1}) over the whole concentration range (up to 40 μM) assuming a rapid and quantitative equilibration of M2a between both halflayers. The reaction enthalpy of $\Delta H^0 = -38.5$ kJ/mol at 45°C is distinctly larger than $\Delta H^0 = -71$ kJ/mol (-17 kcal/mol) at 30°C and can be explained as the sum of the actual binding enthalpy (-63 kJ/mol; expected for ΔH^0 at 45°C, see Wieprecht et al. [9]) and the additional peptide translocation (or pore formation/lipid perturbation) enthalpy of $+25$ kJ/mol. A peptide translocation is in accordance with results obtained by fluorescence resonance energy transfer, which showed that membrane permeabilization is coupled to a translocation of peptide from the outer leaflet to the inner leaflet of the bilayer [29].

5. Conclusions

In the present work we have shown that the lipid affinity of M2a as well as the pore formation activity are very similar for highly curved vesicles (SUVs) and planar membranes (LUVs). Both model systems are hence equally suited to study peptide binding and pore formation. The free energy of binding and the binding constant were almost identical for both model systems. However, both the enthalpy and entropy of binding were distinctly higher for LUVs than for SUVs revealing an entropy–enthalpy compensation mechanism. The enthalpic and entropic differences were traced back to differences in the lipid packing between SUVs and LUVs. Incorporation of the peptide into LUVs leads to a stronger disruption of van der Waals interactions and to a larger increase in the lipid mobility than peptide incorporation into less tightly packed SUVs. The binding isotherms of M2a to POPC/POPG (3:1) SUVs and LUVs could be described by a surface partition model where the peptide concentration at the membrane surface was calculated with the Gouy–Chapman theory. At 45°C a rapid and quantitative equilibration of the peptide occurs between the outer and inner monolayer of the vesicles.

Acknowledgements

We are grateful to Dr W.L. Maloy (Magainin Pharmaceuticals, Inc, Plymouth Meeting, PA) for the generous gift of magainin 2 amide. This work was supported by the Swiss National Science Foundation, Grant 31.42058.94.

References

- [1] M. Zasloff, Magainins, a class of antimicrobial peptides from *Xenopus* skin: isolation, characterization of two active forms, and partial cDNA sequence of a precursor, *Proc. Natl. Acad. Sci. USA* 84 (1987) 5449–5453.
- [2] H.V. Westerhoff, R.W. Hendler, M. Zasloff, D. Juretic, Interactions between a new class of eukaryotic antimicrobial agents and isolated rat liver mitochondria, *Biochim. Biophys. Acta* 975 (1989) 361–369.
- [3] H.V. Westerhoff, D. Juretic, R.W. Hendler, M. Zasloff, Magainins and the disruption of membrane-linked free-

- energy transduction, *Proc. Natl. Acad. Sci. USA* 86 (1989) 6597–6601.
- [4] K. Matsuzaki, M. Harada, S. Funakoshi, N. Fujii, K. Miyajima, Physicochemical determinants for the interactions of magainins 1 and 2 with acidic lipid bilayers, *Biochim. Biophys. Acta* 1063 (1991) 162–170.
- [5] B. Bechinger, M. Zasloff, S.J. Opella, Structure and orientation of the antibiotic peptide magainin in membranes by solid-state nuclear magnetic resonance spectroscopy, *Protein Sci.* 2 (1993) 2077–2084.
- [6] T. Wieprecht, M. Dathe, M. Schumann, E. Krause, M. Beyermann, M. Bienert, Conformational and functional study of magainin 2 in model membrane environments using the new approach of systematic double-D-amino acid replacement, *Biochemistry* 35 (1996) 10844–10853.
- [7] T. Wieprecht, M. Dathe, E. Krause et al., Modulation of membrane activity of amphipathic, antibacterial peptides by slight modifications of the hydrophobic moment, *FEBS Lett.* 417 (1997) 135–140.
- [8] M.R. Wenk, J. Seelig, Magainin 2 amide interaction with lipid membranes: calorimetric detection of peptide binding and pore formation, *Biochemistry* 37 (1998) 3909–3916.
- [9] T. Wieprecht, M. Beyermann, J. Seelig, Binding of antibacterial magainin peptides to electrically neutral membranes: thermodynamics and structure, *Biochemistry* 38 (1999) 10377–10387.
- [10] G. Beschiaschvili, J. Seelig, Peptide binding to lipid bilayers. Nonclassical hydrophobic effect and membrane-induced pK shifts, *Biochemistry* 31 (1992) 10044–10053.
- [11] J.A. Gazzara, M.C. Phillips, S. Lund-Katz et al., Effect of vesicle size on their interaction with class A amphipathic helical peptides”, *J. Lipid Res.* 38 (1997) 2147–2154.
- [12] J. Seelig, P. Ganz, Nonclassical hydrophobic effect in membrane binding equilibria, *Biochemistry* 30 (1991) 9354–9359.
- [13] L.D. Mayer, M.J. Hope, P.R. Cullis, Vesicles of variable sizes produced by a rapid extrusion procedure, *Biochim. Biophys. Acta* 858 (1986) 161–168.
- [14] C.J.F. Böttcher, C.M. van Gent, C. Pries, *Anal. Chim. Acta* 24 (1961) 203–204.
- [15] T. Wiseman, S. Williston, J.F. Brandts, L.N. Lin, Rapid measurement of binding constants and heats of binding using a new titration calorimeter, *Anal. Biochem.* 179 (1989) 131–137.
- [16] J. Seelig, Titration calorimetry of lipid–peptide interactions, *Biochim. Biophys. Acta* 1331 (1997) 103–116.
- [17] R. Aveyard, D.A. Haydon, An introduction to the principles of surface chemistry, Cambridge University Press, London, 1973.
- [18] S. McLaughlin, Electrostatic potentials at membrane–solution interfaces, *Curr. Top. Membr. Transp.* 9 (1977) 71–144.
- [19] S. McLaughlin, The electrostatic properties of membranes, *Annu. Rev. Biophys. Biophys. Chem.* 18 (1989) 113–136.
- [20] C.R. Cantor, P.R. Schimmel, *Biophysical Chemistry*, vol. 1, Freeman, San Francisco, 1980.
- [21] J. Seelig, S. Nebel, P. Ganz, C. Bruns, Electrostatic and nonpolar peptide–membrane interactions. Lipid binding and functional properties of somatostatin analogues of charge $z = +1$ to $z = +3$, *Biochemistry* 32 (1993) 9714–9721.
- [22] T. Wieprecht, O. Apostolov, M. Beyermann, J. Seelig, Thermodynamics of the α -helix-coil transition of amphipathic peptides in a membrane environment: Implications for the peptide–membrane binding equilibrium, *J. Mol. Biol.* 294 (1999) 785–794.
- [23] F. Tanford, *The hydrophobic effect: formation of micelles and biological membranes*, Wiley & Sons, New York, 1980.
- [24] Y.H. Chen, J.T. Yang, H.M. Martinez, Determination of the secondary structures of proteins by circular dichroism and optical rotatory dispersion, *Biochemistry* 11 (1972) 4120–4131.
- [25] K. Matsuzaki, O. Murase, H. Tokuda, S. Funakoshi, N. Fujii, K. Miyajima, Orientational and aggregational states of magainin 2 in phospholipid bilayers, *Biochemistry* 33 (1994) 3342–3349.
- [26] S. Ludtke, K. He, H. Huang, Membrane thinning caused by magainin 2, *Biochemistry* 34 (1995) 16764–16769.
- [27] M. Bloom, E. Evans, O.G. Mouritsen, Physical properties of the fluid lipid-bilayer component of cell membranes: a perspective, *Q. Rev. Biophys.* 24 (1991) 293–397.
- [28] R.J. Davies, M.N. Jones, The thermal behaviour of phosphatidylcholine-glycophorin monolayers in relation to monolayer and bilayer internal pressure, *Biochim. Biophys. Acta* 1103 (1992) 8–12.
- [29] K. Matsuzaki, O. Murase, N. Fujii, K. Miyajima, Translocation of a channel-forming antimicrobial peptide, magainin 2, across lipid bilayers by forming a pore, *Biochemistry* 34 (1995) 6521–6526.